Prediction of submerged landslide generated waves in dam reservoirs: an applied approach

B. Ataie-Ashtiani
A. Najafi-Jilani
Department of Civil Engineering
Sharif University of Technology
Tehran
Iran

Abstract
Impulsive waves in dam reservoirs may be generated by any type of geophysical mass flow, including debris flows, debris avalanches, landslides, and rock falls. This phenomenon may be endangering the dam stability, human life and devastating downstream cities. The estimation of the landslide generated waves amplitude is of the utmost importance in dam engineering and water reservoir planning. In this work, a higher order Boussinesq-type numerical model is applied to study the sensitivity of the wave amplitude to the landslide geometry and kinematics. The numerical results are also used to provide an engineering estimation method to predict the landslide generated wave amplitude in dam reservoir using the landslide geometry parameters and water body conditions. The estimation method is verified and proven by comparison of the results with several experimental and real cases.

Keywords: Dam reservoir, submerged landslide, impulsive waves, landslide, Boussinesq model, Numerical model

1. Introduction
Underwater landslides in artificial reservoirs can trigger local impulsive waves with high run-up, endangering dam stability, human life and devastating downstream cities. Submarine landslides, which often accompany large earthquakes, can disturb the overlying water column as sediment and rock slump down slope. Any sort of geophysical mass flow, including debris flows, debris avalanches, landslides, and rock falls can generate submarine landslide impulsive waves. Estimating the amplitude of Landslide Generated Waves (LGW) is of the utmost importance in dam engineering and water reservoir planning. There are a several real cases in which the LGWs destroy the dam or the villages around it. For instance a landslide on October 9, 1963 with a volume of 270 million m^3 generated an impulse wave initially more than 70m tall in Vaiont dam reservoir in Italy, the worlds' tallest double thin arch dam. The impulse wave completely

destroyed five villages and about 2500 people were killed. Other examples of large impulse waves generated by landslides are known from Lituya Bays, Alaska [18]; Yanahuin Lake, Peru; and Shimabara Bay in Japan [21].

The numerical modelling and experimental investigations have been developed to predict the impulse wave characteristics. An overview of numerical modelling of landslide waves is presented in Table 1. A major part of this body of works is related to landslide tsunami waves which are a special type of tsunami waves caused by slope instability. As it can be seen, the submarine landslide generated tsunami is fairly well investigated but the application of impulse wave models for forecasting the submerged LGW characteristics in dam reservoirs still requires further studies. In addition to the numerical studies, experimental investigations have been performed with regards to LGWs. An overview of laboratory works related to this topic is presented in Table 2. It can be seen in this table that most experimental works are related to submarine landslide generated tsunami. The basic parameters in experiments consist of bed slope, geometry and initial submergence of failure mass and particularly the laws of motion of submerged body are set in accordance with landslide tsunamis. Moreover, the conclusion of empirical formulations is specially made and verified for tsunami applications. For instance, the recent studies on landslide generated tsunamis performed by Grilli et al. in 2005 [8] has a main constraint for bed slope as $\theta < 30°$ or in other recent works presented by Panizzo et al. in 2005 [22] the maximum bed slope is fixed on $\theta = 36°$ and it focused on sub-aerial landslide. There are noticeable constraints in other geometrical specification of landslide and characteristics of water body when using landslide tsunami predictive methods in a dam reservoir. Thus, more research is required for forecasting the main characteristics of impulse wave caused by landslide in dam reservoir, where the bed slope may be much steeper than the inclined sea floor and the water depth, location of failure mass, propagation distances and water body specifications are seriously different from ocean.

In this work, an extended higher order Boussinesq-type model is used to provide a simple engineering estimation method for prediction of impulse wave amplitude caused by underwater landslide in dam reservoirs. The main information required consists of landslide geometry and water body conditions. The sensitivity analysis of wave amplitude is also made here using numerical results. The Mathematical formulation of the model is an extension of (4,4) Padé approximant [4] to include moving bottom boundary to be applicable to study LGWs. The details of derivation for extended formulations as well as numerical modelling, calibration and verification of model are clearly presented in Reference [1].

2. Mathematical formulation

The mathematical formulation of the numerical model used in this work is developed based on fourth order Boussinesq-type equations, known as (4,4) Padé approximant [4].

No.	Reference	Ref	Numerical Model Name	Governing equations	Numerical method	Model dimensions	Failure Mass	Wave simulation stage	Experimental validation	Real case study
1	Noda (1971)	[19]	–	NSW	FDM	Depth averaged	Rigid sliding	Generation	Done	–
2	Mader (1973)	[17]	ZUNI	NSW	FDM	Width averaged	Rigid sliding	Gen., Prop., run-up	Done	–
3	Raney/Butler (1975)	[25]	–	NSW	FDM	Depth averaged	Rigid sliding	Gen., Prop., run-up	–	Landslide Tsunami
4	Goto/Ogawa (1992)	[5]	TIME	BW	FDM	Depth averaged	Rigid sliding	Gen., Prop., run-up	–	Landslide Tsunami
5	Jiang/Leblond (1992)	[12]	–	NSW Viscous flow	FDM	Three dimensional	Mudslide	Gen., Prop.	Done	Landslide Tsunami
6	Titov (1997)	[29]	MOST	NSW	FDM	Depth averaged	Rigid sliding	Gen., Prop., run-up	–	Landslide Tsunami
7	Rzadkiewicz et al (1997)	[26]	Nasa-Vof2d	Potential flow Bingham Rheology	FDM	Width averaged	Slumping	Generation	Done	–
8	Grilli et al (1999)	[9]	GW-2D	Potential flow	BEM	Width averaged	Rigid sliding	Generation	Done	Landslide Tsunami
9	Imran et al (2001)	[11]	–	NSW Herschel-Bulkley Rheology	FDM	One dimensional	Slumping	Generation	Done	–
10	Synolakis et al (2002)	[28]	TUNAMI	LSW	BEM	Depth averaged	Rigid sliding	Gen., Prop.	–	Landslide Tsunami
11	Grilli et al (2002)	[6]	BIEM	Potential flow	BEM	Three dimensional	Rigid sliding	Gen., Prop.	Done	–
12	Watts et al (2003)	[32]	GEOWAVE	BW	BEM	Three dimensional	Sliding/slump.	Gen., Prop., run-up	Done	Landslide Tsunami
13	Grilli/Watts (2003)	[7]	BING	BW Bingham Rhe.	BEM	Width averaged	Slumping	Gen., Prop.	Done	–
14	Lynett/Liu (2004)	[16]	COULWAVE	BW-Multi Layer	FDM	Depth averaged	Slumping	Gen., Prop., run-up	Done	Landslide Tsunami
15	Panizzo et al (2005)	[22]	–	Potential flow	SPH	Three dimensional	Slumping	Gen., Prop.	Done	Landslide wave in res.
16	Ataie/Jilani (2006)	[1]	–	BW	FDM	Depth averaged	Sliding/slump.	Gen., Prop.	Done	–

NSW: Nonlinear Shallow Water Wave Equations; LSW: Linear Shallow Water Wave Equations; BW: Boussinesq-type Wave Equations
Gen: Generation; Prop: Propagation
BEM: Boundary Element Method; FDM: Finite Difference Method; SPH: Smooth Particle Hydrodynamics

Table 1: An overview of the main numerical investigations of impulsive waves caused by landslide

The model includes the moving bottom boundary. The extension procedure is a forward step of the Lynett & Liu approach [15] which was used for extension of second-order Boussinsq wave equations. A schematic of the main geometric parameters is shown in Figure 1. The dimensionless form of governing equations and boundary conditions in three-dimensional domain can be described as [15]:

$$\mu^2\nabla.u + w_z = 0 \qquad \text{on} \quad -h \le z \le \varepsilon.\zeta \quad \text{(Continuity equation)} \tag{1}$$

$$u_t + \varepsilon u\nabla.u + \frac{\varepsilon}{\mu^2} w u_z = -\nabla p \qquad \text{on} -h \le z \le \varepsilon.\zeta \tag{2}$$

(Momentum Equation in 2 horizontal dir.)

$$\varepsilon w_t + \varepsilon^2 u.\nabla w + \frac{\varepsilon^2}{\mu^2} w w_z = -\varepsilon P_z - 1 \qquad \text{on} -h \le z \le \varepsilon.\zeta \tag{3}$$

(Momentum equation in z dir.)

$$w = \mu^2 (\zeta_t + \varepsilon.u.\nabla\zeta) \qquad \text{on } z = \varepsilon.\zeta \quad \text{(KFSBC)} \tag{4}$$

$$p = 0 \qquad \text{on} \quad z = \varepsilon.\zeta \quad \text{(DFSBC)} \tag{5}$$

$$w + \mu^2 u.\nabla h + \frac{\mu^2}{\varepsilon} h_t = 0 \qquad \text{on} \quad Z = -h \quad \text{(BBC)} \tag{6}$$

where x and y are the horizontal coordinates scaled by l_0 which is the horizontal length scale, z is the vertical coordinate scaled by h_0 which is the characteristic water depth, t is time and scaled by $l_0/(gh_0)^{1/2}$, θ is the water surface displacement scaled by a_0 which is the impulse wave amplitude, h is the total depth based on still water considering the moving bottom boundary ($h(x,y,t)$) and scaled by h_0, **u** is the vector of horizontal velocity components (u,v) scaled by $(\varepsilon(gh_0)^{1/2}$, w is the velocity in vertical direction scaled by $(\varepsilon/\mu).(gh0)^{1/2}$, p is the water pressure scaled by γa_0, and ∇=($\partial/\partial x$, $\partial/\partial y$) is the horizontal gradient vector. The subscripts denote the partial derivative. The non-linearity and dispersion parameters are $\varepsilon = a_0/h_0$ and $\mu = h_0/l_0$, respectively. The no-flow condition is assigned for lateral boundaries and the numerical simulation shall be stopped before the generated waves are received by lateral boundaries. In perturbation analysis, the velocity domain components "u" and "w" shall be expanded in to [15]:

$$u = u_0 + \mu^2 u_1 + \mu^4 u_2 \tag{7}$$

$$w = \mu^2 w_1 + \mu^4 w_2 \tag{8}$$

No	Reference	Ref No	Wave Tank/Flume Specifications L(m)	W(m)	H(m)	Bed slope (deg)	Failure Mass specifications	Impluse Mechanism	Model Dimensions	Wave Simulation Stage	Slide Location	Comparison with num Data	Notes
1	Jonson/Bermel (1949) Wiegel (1955) Prins (1958)	[13] [34] [24]	Shallow Water Tank			–	Steel plate	Rigid Crashing	–	Generation	Sub-aerial		–
2	Kamphuis/Bowering (1972)	[14]	Shallow Water Tank			45	Steel box	Rigid sliding	–	Generation	Sub-aerial		Definition of compact Froude No
3	Heinrich (1992)	[10]	4.0	0.3	2.0	45 30	Triangle solid block (50x50cm)/ Gravel with Identical Dia	Rigid/ Slumping mass	Flume/2VD (two-vertical dimension)	Generation	Submerged	Done	–
4	Watts (1998)	[31]	9.14	0.101	0.66	45	PVC Triangle Solid Block (86x86cm)	Rigid	Flume/2VD	Generation	Submerged	–	Presentation of wave Maker Curves as a function of solid slide and water spec.
5	Grilli/Watts (2005)	[8]	30	3.6	1.8	30 15 13.85 5	Semi-Ellipse Aluminium Sheet	Rigid Sliding	Tank /2VD	Gen., Prop.	Submerged	Done	Wave absorber system installed at lateral boundaries
6	Walder et al (2003)	[30]	3.0	0.285	1.0	19.5 15 11.2	Hollow Rect. Nylon box with triangle snout	Rigid Sliding	Flume /2VD	Generation	Sub-aerial	Done	Empirical formulations for sub-aerial impulse wave estimation
8	Enet et al. (2003)	[2]	30	3.6	1.8	15	Aluminium sheet with Geometry of of truncated hyperbolic secant func.	Rigid Sliding	Tank /3D	Gen., Prop.	Submerged	Done	Verification of BIEM as a 3D potential flow model
9	Watts et al (2003)	[32]	30	3.6	1.8	45	Different granular materials with 3mm dia. consist of glass beads, steel shots & lead shot	Slumping mass	Flume/2VD	Generation	Submerged	Done	–
7	Fritz et al (2004)	[3]	11	0.5	1.0	45	Failure soil mass caused by Pnematic Landslide Generator	Slumping mass	Flume/2VD	Gen., Prop.	Sub-aerial	–	Categorisation of impulse wave caused by landslide
10	Panizzo et al (2005)	[22]	11.5	6	0.8	16 26 36	Solid rectangular box	Rigid crashing	Tank/3D	Gen., Prop. and run-up	Sub-aerial	Done	Empirical formula. for sub-aerial landslide waves in dam reservoirs

***Table 2:** An overview of the main laboratory investigations of impulsive waves caused by landslide*

μ^2 is the basic small parameter in analysis. Using perturbation analysis and substituting an expanded form of velocity components into governing equations and boundary conditions, the main three equations, Equations (9) and (10) (considering (10) is a two-component vector equation) that describe the water surface response to the bottom displacement are concluded as follow. The details of derivation are presented in Reference [1].

$$
\begin{aligned}
\frac{1}{\varepsilon} h_t + \zeta_t + \nabla.\{ & (\varepsilon\zeta + h)\mathbf{u}_0 \\
& + \mu^2 [\tfrac{-1}{6}(\varepsilon^3\zeta^3 + h^3)A + \tfrac{1}{2}\tilde{z}^2(\varepsilon\zeta + h)A - \tfrac{1}{2}(\varepsilon^2\zeta^2 - h^2)(\nabla.B) + \tilde{z}^2(\varepsilon\zeta + h)(\nabla.B)] \\
& + \mu^4 [\tfrac{1}{120}(\varepsilon^5\zeta^5 + h^5)\nabla(\nabla.A) - \tfrac{1}{24}(\varepsilon\zeta + h)\tilde{z}^4\nabla(\nabla.A) - \tfrac{1}{12}(\varepsilon^3\zeta^3 + h^3)\nabla(\nabla.(\tilde{z}^2.A) \\
& + \tfrac{1}{4}(\varepsilon\zeta + h)\tilde{z}^2\nabla(\nabla.(\tilde{z}^2 A)) + \tfrac{1}{24}(\varepsilon^4\zeta^4 - h^4)\nabla(\nabla.(\nabla B)) - \tfrac{1}{6}(\varepsilon\zeta + h)\tilde{z}^3\nabla(\nabla.(\nabla B)) \\
& - \tfrac{1}{6}(\varepsilon^3\zeta^3 + h^3)\nabla(\nabla.(\tilde{z}\nabla B)) + \tfrac{1}{2}(\varepsilon\zeta + h)\tilde{z}\nabla(\nabla.(\tilde{z}\nabla B)) \\
& + \tfrac{1}{2}(\varepsilon^2\zeta^2 - h^2)\nabla C - (\varepsilon\zeta + h)\tilde{z}\nabla C] \} = O(\varepsilon^6, \mu^6)
\end{aligned}
\tag{9}
$$

$$
\begin{aligned}
\mathbf{u}_{0t} + \varepsilon(\nabla.\mathbf{u}_0)\mathbf{u}_0 + \varepsilon & \left(w_1|_{z=0}\right)\mathbf{u}_{0z} \\
& + \mu^2 \left[\mathbf{u}_{1t}|_{z=0} + \varepsilon(\nabla.\left(\mathbf{u}_1|_{z=0}\right))\mathbf{u}_0 + \varepsilon(\nabla.\mathbf{u}_0)\left(\mathbf{u}_1|_{z=0}\right) + \varepsilon\left(w_2|_{z=0}\right)\mathbf{u}_{0z} + \left(w_1|_{z=0}\right)\left(\mathbf{u}_{1z}|_{z=0}\right)\right] \\
& + \mu^4 \left[\mathbf{u}_{2t}|_{z=0} + \varepsilon(\nabla.\left(\mathbf{u}_2|_{z=0}\right))\mathbf{u}_0 + \varepsilon(\nabla.\left(\mathbf{u}_1|_{z=0}\right))\left(\mathbf{u}_1|_{z=0}\right) + \varepsilon(\nabla.\mathbf{u}_0)\left(\mathbf{u}_2|_{z=0}\right) \right. \\
& \left. + \varepsilon\left(w_2|_{z=0}\right)\left(\mathbf{u}_{1z}|_{z=0}\right) + \left(w_1|_{z=0}\right)\left(\mathbf{u}_{2z}|_{z=0}\right)\right] \\
& + \nabla\left(P|_{z=0}\right) = 0\,(\varepsilon^6, \mu^6)
\end{aligned}
\tag{10}
$$

where vector $A = \nabla.(\nabla.\mathbf{u}_0)$, scalar $B = \nabla.(h\mathbf{u}_0) + h_t/\varepsilon$ and $\tilde{z}$ is a weighted average of two distinct characteristic water depth as described by Gobbi et al. [4]. The above equations are solved simultaneously to obtain the main three variables u, v (horizontal velocity components) and ζ (water wave elevation). A numerical model has been developed based on this set of equations using finite difference method to simulate the impulsive wave generation and propagation. The sixth order difference scheme and discretization method is applied following Gobbi et al., [4] numerical model but the moving bottom boundary is included here.

3. Wave amplitude sensitivity analysis

As shown in Figure 1, two main categories of parameters can be recognised which affected the landslide impulse waves. The first category includes parameters which are related to the geometry of the failure mass and sloping bed. These characteristics consist of bed slope; θ, the length of sliding block along the slope; B, the maximum thickness of sliding block; T, the initial still water depth at the mass center point of sliding mass; h_{0C}, and the sliding soil density; γ. The second category is the generated wave characteristics such as amplitude (or maximum depression); a_0, wavelength, and period. It is convenient to define the basic dimensionless parameters that describe the landslide and its location. Based on laboratory investigations [5], two dimensionless ratios can be defined which describe the mass failure geometric and its initial location as follows: Maximum thickness (T) over the length of sliding block along the slope (B); (i.e. T/B), and the initial submergence of failure mass (h_{0C}) over its length (B); (i.e. h_{0C}/B). Another non-dimensional parameter can be defined using maximum depression of water surface (a_0) divided by a characteristic length. This characteristic length is named as S_0 and defined as [9]:

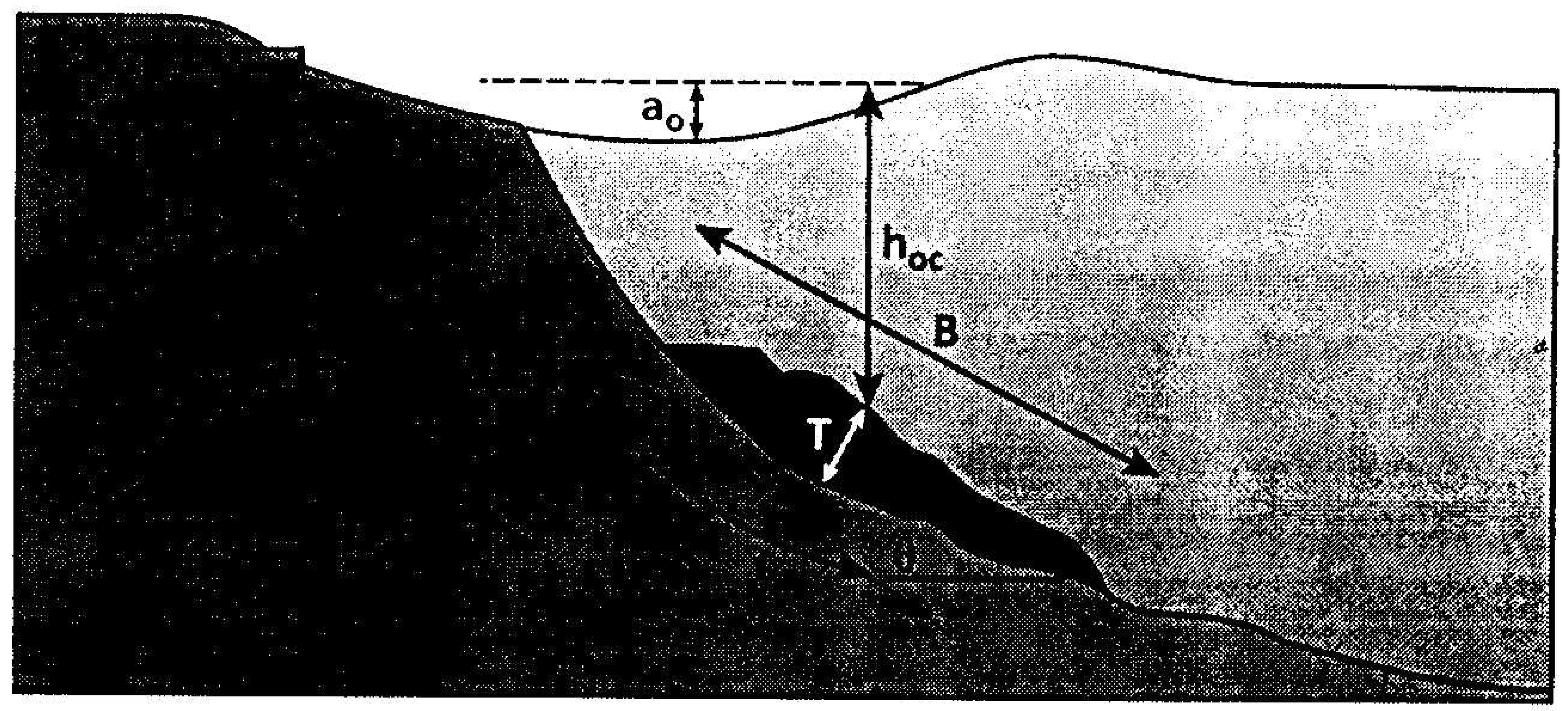

Figure 1: A schematic of main geometric parameters in submerged landslide generated impulse wave

$$S_0 = \frac{u_t^2}{\alpha_0} \text{ where } u_t = \sqrt{g.B}.\sqrt{\frac{\pi(\gamma - 1)}{2C_d}.\sin\theta} \qquad \text{and} \quad a_0 = g.\frac{\gamma - 1}{\gamma + C_m}\sin\theta \tag{11}$$

In this equation, ut is the terminal velocity of failure mass, α_0 is its initial acceleration and C_d and C_m are the shape related coefficients of failure mass consist of drag and added mass coefficients, respectively. For investigation of influences of various parameters on impulse wave amplitude, the numerical results in various conditions are presented as a set of graphs in Figure 2. In this Figure, the interaction of landslide geometry and wave amplitude can be seen. The results presented for different values of bed slope; θ, consist of 5, 15, 30 and 45 degrees. The range of variation of dimensionless parameters is selected based on observed underwater landslide in real cases and available experimental characteristics. Some of these specifications are mentioned in section 4. As it can be seen, in a constant value of bed slope, the wave height will be increased when the initial submergence of failure mass diminishes or the sliding block thickness increases. The effects of the thickness of sliding block increases in shallower sliding. When the bed slope increases, the sliding velocity and its acceleration will be increased and the impulsive wave amplitude will be enlarged. For further investigation, the effect of bed slope on the impulsive wave generation and propagation are discussed. As can be seen in Figure 3, the wave amplitude increases when the bed slope enlarges. In Figure 3, the wave propagation pattern can be seen at three time stages. All of the conditions consisting of landslide geometry and kinematics as well as failure mass density are identical in all cases. The numerical wave tank dimensions assume 8x8 meters. The geometric ratio of sliding block is supposed as T/B=0.1 and the initial submergence of sliding block ratio; h_{0C}/B=1. For Figures 3a, 3c, and 3e; the bed slope is assumed θ=5° and for figures b, d, and f; θ=10°. In constant geometrical and kinematics specifications, the bed slope influences on the impulsive wave generation and propagation can be observed in Figure 3. The wave heights are multiplied by 10, for a better recognition in the figures. The wave height near to the source of the landslide is influenced intensively by bed slope rather than far from it. Furthermore, it seems that the wave length as well as wave propagation speed and wave group velocity increase in steeper slope landslide at least in near field.

4. Wave amplitude prediction method

The numerical simulation results that are used for sensitivity analysis and illustrated in Figure 2 can be applied for estimating the amplitude of impulsive wave caused by an underwater landslide in a dam reservoir. The basic parameters which should be known to use the estimation method are listed here: 1) The geometric parameters of sliding mass consist of slide length along the bed slope (B), maximum thickness of failure mass (T), and initial submergence at the mass center (h_{0C}). 2) The characteristic length of motion; S_0 which is defined in equation (11). Based on this equation, the sliding mass density as well as the shape related coefficients of failure mass consists of drag and added mass coefficients (C_d and C_m, respectively) should be defined. Definition of the coefficients in real case problems can be carried out using empirical methods based on the shape and dimensions of sliding mass. It must be noted that the range of validity of presented prediction method is $\gamma \in [1.8, 2.1]$ where γ is the failure mass density.

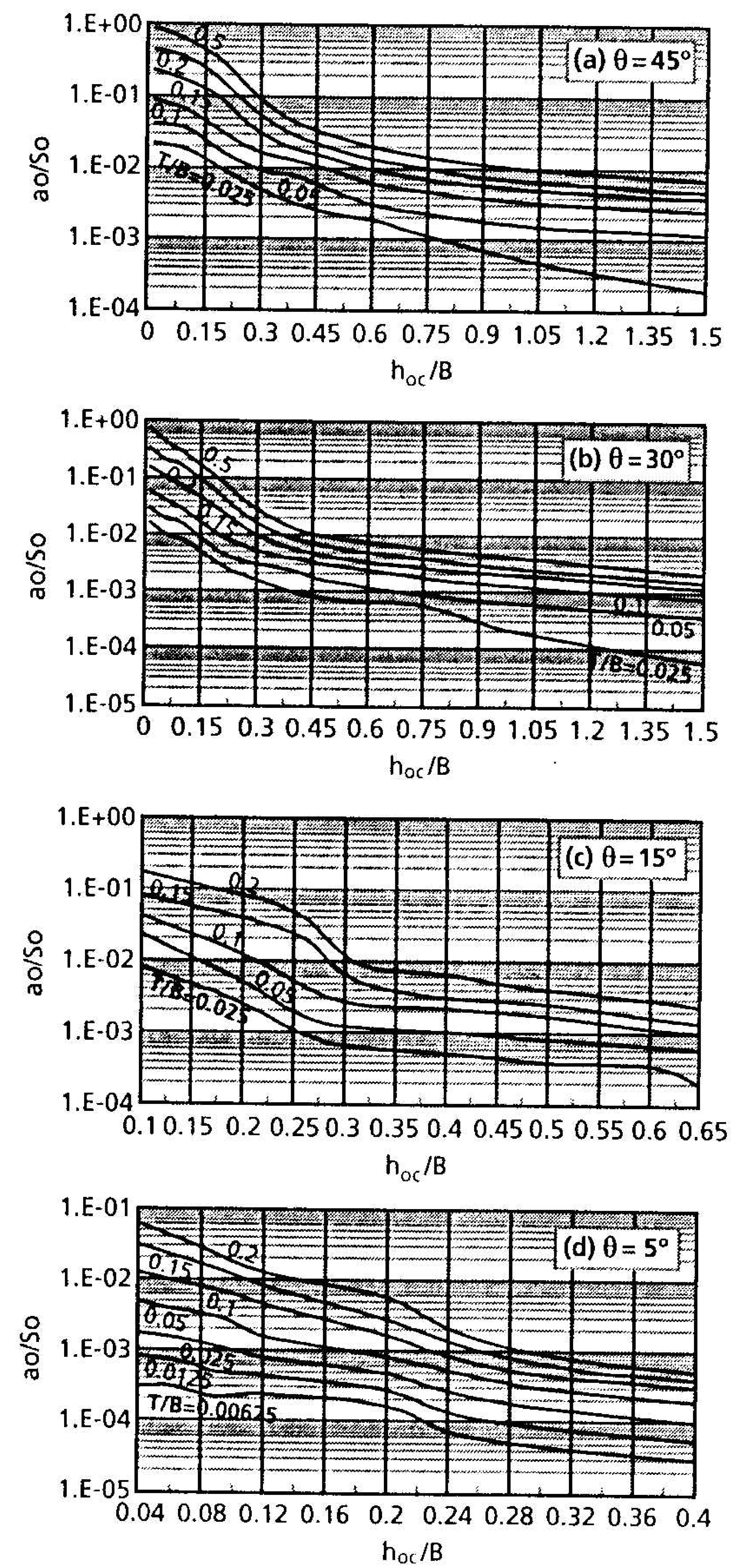

Figure 2: Impulse wave amplitude (a_o) vs. landslide geometry and water body conditions, the bed slope; θ = a)45°, b) 30°, c) 15° and d) 5°, h_{OC} is the initial submergence of landslide, B is the landslide length along the inclined bed, T is the maximum thickness of landslide and S_0 is the characteristic length of the landslidemotion which is defined in Equation 11.

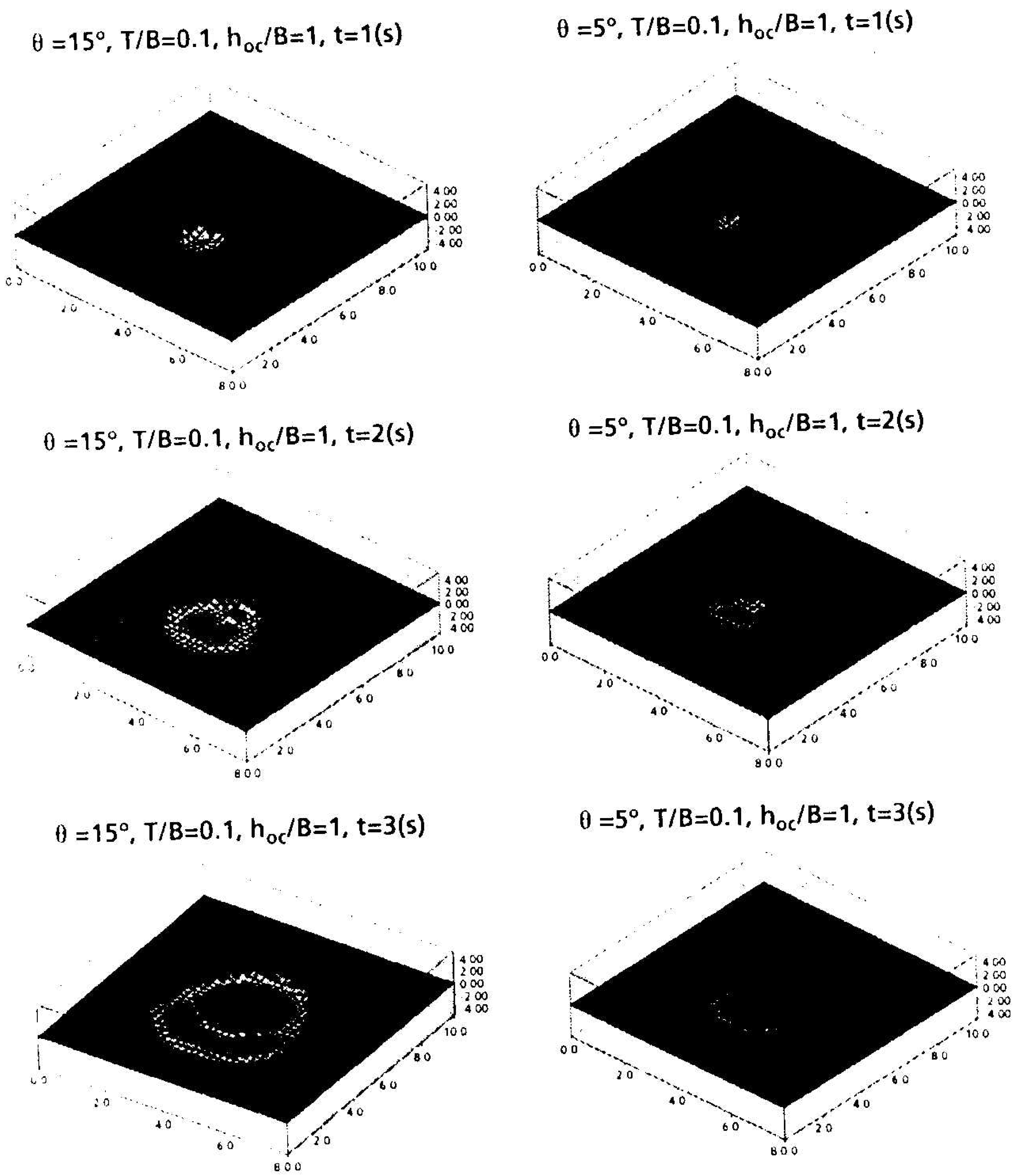

Figure 3: Numerical results for impulsive wave amplitude in depth integrated model to evaluate the influence of bed slope on the wave height and propagation pattern, in all cases the ratios T/B and h_{0C}/B is assumed 0.1 and 1; respectively, $C_d = 1$, $C_m = 1$, $\gamma = 1.85$, the wave heights multiplied for better display

4.1. Validation of prediction method

4.1.1 Comparison with experimental data

In this section, some available experimental measurements are used to validate the presented prediction method. The estimated impulse wave amplitude is compared with laboratory measurements in several cases. The experimental data that are used to validate the presented estimation method are selected from Table 2. The comparison is made with laboratory data obtained from experiments in which the impulsive wave caused by submerged sliding mass and the constraint of landslide density described later is satisfied. All of the experimental specifications and the procedure of prediction method are presented in Table 3. In this Table, the sliding mass geometry, failure mass density and landslide kinematics are listed. All of the experimental data are obtained from the corresponding reference mentioned in Table 3. Moreover, the basic dimensionless ratios that are used in the presented prediction method are determined in this Table. The description of experiments in each case is discussed briefly in Table 2. The comparison of predicted wave amplitude and the measured data are seen in the last columns of Table 3. As it is shown, the prediction error is about 5% and it confirms a good reliability of presented prediction method.

In Grilli et al's experiments [6], the submerged sliding block is a semi-ellipse solid sheet and equation (11) can be used for the determination of slide kinematics parameters consisting of terminal velocity (u_t) and initial acceleration (α_0). A schematic of their experimental tank is shown in Figure 4. The law of motion for underwater sliding block is similar to the real case condition of submerged landslide [30]. Thus in real cases, equation (11) can be used to apply presented prediction method for estimation of impulse wave amplitude. The use of the prediction method in some real cases is discussed in the next sections. It must be noted that for laboratory works of Watts (1998) [31] and Heinrich (1992) [10], because the sliding mass is a solid triangle block, equation (11) can not be used for determination of u_t and α_0, thus the measured data of these kinematics parameters are used in prediction procedure. Figure 4 shows also a schematic of these experiments and adefinition of landslide geometric parameters in these cases. The dimensions and other specifications of these laboratory cases are presented in Table 2. The use of basic parameters to predict the impulse wave amplitude and comparison with experimental data is presented in Table 3. As seen, in spite of different shape of landslide in these cases, the present method works very well.

4.1. 2. Comparison with 3D numerical models

In this section, presented prediction method is compared with BIEM numerical model as a three dimensional fully nonlinear potential flow model. The high degree of its accuracy in simulating of a submerged landslide impulse wave is well documented [8, 9]. All of the numerical cases properties are listed in Table 4. The BIEM results are directly obtained from Watts et al. (2005) [33]. We use the numerical results of BIEM to validate presented prediction method. The specifications of BIEM are listed in Table 1.

Ref no	Reference	Landslide specifications					Water body spec.		Landslide kinematrics			Basic ratios		Predicted ratio-fig 2	Predicted amplitude	Measured amplitude	Error
		$B(m)$	$T(m)$	C_m	C_d	γ	$\theta(deg)$	$h_{0c}(m)$	$u_t(m/s)$	$a_0(m/s^2)$	$S_0(m)$	T/B	h_{0c}/B	a_0/S_0	a_{0P} (m)	a_{0M} (m)	%
[6]	Grilli et al. (2002)	1	0.052	1.76	1.53	1.81	15	0.261	1.45	0.576	3.65	0.052	0.261	0.0014	0.0051	0.0052	1.9
[31]	Watts (1998)	0.121	0.0608	0.81	1.67	2.1	45	0.074	0.65	1.95	0.21	0.5	0.611	0.02	0.0042	0.0045	6.6
[31]	Watts (1998)	0.121	0.0608	0.75	1.75	1.9	45	0.059	0.56	1.63	0.19	0.5	0.49	0.03	0.0057	0.0055	3.6
[10]	Heinrich (19920	0.707	0.353	–	–	2	45	0.01	0.6	1.5	0.24	0.5	0.014	0.92	0.22	0.22	0.1

Table 3: *Experimental validation of presented prediction method, the main specifications of experiments are mentioned in Table 2*

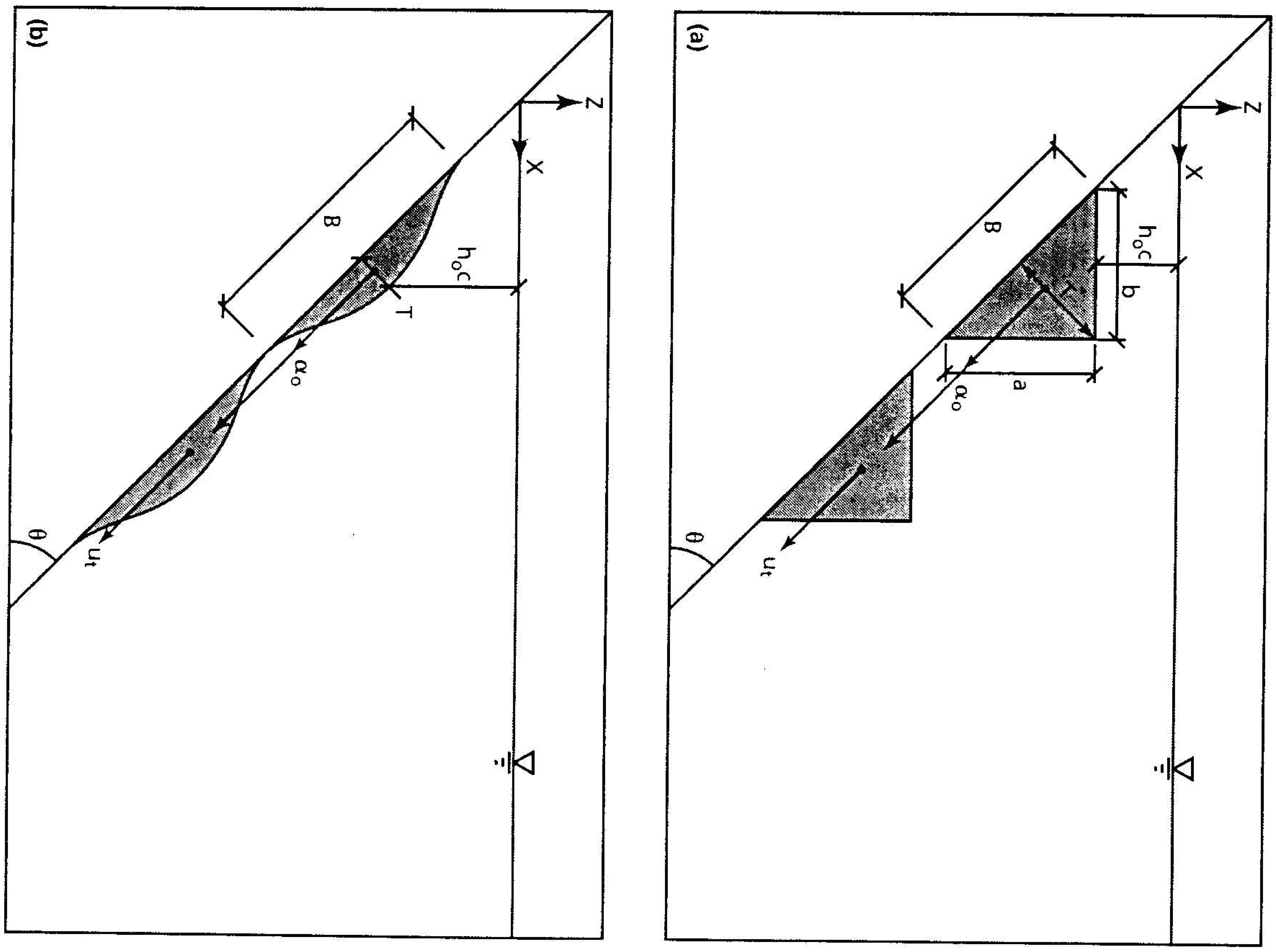

Figure 4: *Schematic of experimental wave tank with different shape of submerged sliding box, a) Watts; 1998 [31] and Heinrich; 1992 [10] and b) Grilli et al., (2002) [6], the prediction method presented here is in a good agreement with both different experiments, the detail of comparison is listed in Table 3*

No	Landslide specifications					Water body spec		Landslide kinematics			Basic ratios		Predicted ratio (fig 2)	Predicted amplitude	BIEM amplitude	Error
	$B(m)$	$T(m)$	C_m	C_d	γ	$\theta(deg)$	$h_{0C}(m)$	$u_t(m/s)$	$a_0(m/s^2)$	$S_0(m)$	T/B	h_{0C}/B	a_0/S_0	$a_{0P}(m)$	$a0M\ (m)$	%
1	1	0.017	1	1	1.85	5	0.087	1.067	0.255	4.47	0.017	0.087	0.0008	0.0035	0.0035	0
2	1	0.017	1	1	1.85	5	0.06	1.067	0.255	4.47	0.017	0.06	0.0013	0.0058	0.0059	1.7
3	1	0.017	1	1	1.85	5	0.17	1.067	0.255	4.47	0.017	0.17	0.0004	0.0017	0.0016	6.2
4	1	0.008	1	1	1.85	5	0.087	1.067	0.255	4.47	0.008	0.087	0.00034	0.0015	0.0016	6.1
5	1	0.013	1	1	1.85	5	0.087	1.067	0.255	4.47	0.013	0.087	0.00053	0.0024	0.0025	4
6	1	0.025	1	1	1.85	5	0.087	1.067	0.255	4.47	0.025	0.087	0.0011	0.0049	0.005	2
7	1	0.052	1	1	1.85	15	0.5	1.84	0.757	4.47	0.052	0.5	0.0019	0.0085	0.009	5.5
8	1	0.052	1	1	1.85	15	0.625	1.84	0.757	4.47	0.052	0.625	0.00088	0.0039	0.0038	2.6
9	1	0.052	1	1	1.85	15	0.259	1.84	0.757	4.47	0.052	0.259	0.00062	0.00277	0.0029	4.5
10	1	0.025	1	1	1.85	15	0.259	1.84	0.757	4.47	0.025	0.259	0.00095	0.0042	0.0043	2.3
11	1	0.075	1	1	1.85	15	0.259	1.84	0.757	4.47	0.075	0.259	0.0028	0.0125	0.0132	5.3
12	1	0.1	1	1	1.85	15	0.259	1.84	0.757	4.47	0.1	0.259	0.004	0.0179	0.0178	0.6
13	1	0.1	1	1	1.85	30	0.5	2.55	1.46	4.47	0.1	0.5	0.003	0.0134	0.0142	5.6
14	1	0.1	1	1	1.85	30	0.75	2.55	1.46	4.47	0.1	0.75	0.0019	0.0085	0.0083	2.4
15	1	0.1	1	1	1.85	30	1	2.55	1.46	4.47	0.1	1	0.0013	0.0058	0.0059	1.7
16	1	0.1	1	1	1.85	30	1.5	2.55	1.46	4.47	0.1	1.5	0.00083	0.0037	0.0037	0
17	1	0.05	1	1	1.85	30	0.5	2.55	1.46	4.47	0.05	0.5	0.0015	0.0067	0.0069	2.9
18	1	0.2	1	1	1.85	30	0.5	2.55	1.46	4.47	0.2	0.5	0.0068	0.0304	0.03	1.3

***Table 4:** Comparing presented prediction method with BIEM numerical model results [8] as a fully nonlinear potential flow model, the main specifications of BIEM numerical model are mentioned in Table 1*

Table 4 shows the comparison of BIEM and presented prediction method. As it is shown, the results of simple prediction method are in a good agreement with BIEM numerical results. The predicted impulse wave amplitude caused by under water landslide has a maximum deviation from 3D numerical model as 5% and it confirm an excellent reliability of presented engineering estimation method to predict the impulse wave amplitude in a water body. The details of the prediction procedure and the basic dimensionless ratios that is used in the prediction method are listed in Table 4. The comparison of results can be seen in the last columns in this table.

4.2. Application of prediction method in some real cases

Most observations and real case studies about underwater landslide generated waves are related to the tsunamis which were caused by submarine mass failure. Thus, although the presented estimation method is developed based on dam reservoir characteristics and checked in different condition by experimental and other numerical data, for additional evaluation of prediction method it is applied in some real cases of submarine LGWs.

4.2.1. The 1946 Unimak, Alaska submarine landslide

More than half a century later, scientists are beginning to piece together the puzzle of an April 1, 1946 wave that killed 159 people in Hawaii, smashed into the Marquesas Islands and kept going to Antarctica. The outcome of investigations is that the most scientists believe that the waves were caused by a submarine landslide, presumably, triggered by the shaking of the initial earthquake. Based on the results of investigations, the geometry of submarine failure mass can be defined by the parameters presented here [32]: the bed slope is 4.3°, the sliding soil density is 1.85, the length along the bed is 40,000m and the thickness is 300m. The initial submergence depth is 1600m. The results come from Figure 2 for T/B=0.0075 and h_{0C}/B=0.042 is a_0/S_0=-0.0004. Assuming that the shape related coefficients of sliding mass consist of added mass and drag coefficients are both equal to one and using equation (11) for determination of S_0, the impulsive wave amplitude estimated as 71.6m can be compared with other numerical models which result in the value of 64m [32]. The comparison shows acceptable reliability of prediction method presented here. It must be mentioned that the estimation graph used in this case is according to bed slope θ=5° although the bed slope in the real case is θ=4.3°.

4.2.2. The 1994 Skagway, Alaska submarine landslide

The impulse wave of November 3, 1994 in Skagway, Alaska, was generated by an underwater landslide formed during the collapse of a cruise ship wharf undergoing construction at the head of Taiya Inlet. The impulsive waves could be caused by two distinct landslides with the geometric and kinematics of them listed here [32]: For slide A; the angle of bed slope is 26°, the soil density is 1.85, the length and thickness are 180 and 20m, respectively. The initial submergence is 24m and the shape coefficients are unit. It can be obtained that the characteristic length S_0=807m, T/B=0.11 and h_0C/B=0.13. Using Figure 2, the ratio a_0/S_0=-0.023 can be acquired and the wave amplitude obtained 18.5m. It can be compared with the obtained numerical results of [32]; 17.3m. The estimated value is acceptable considering that the bed slope in real case (i.e. θ=26°) is less than the bed slope in Figure 2 (i.e. θ=30°). For slide B; bed angle is 22°, the length of sliding block is 215m and its thickness is 15m and the initial submergence is 95. The parameter S_0 can be determined as 964m and the basic dimensionless ratios; T/B and h_{0C}/B as 0.07 and 0.44, respectively. Using Figure 2, it can be obtained that a_0/S_0=-0.0025 and it leads to wave amplitude 2.4m. Comparing predicted and other numerical result [32] that is 2.06m, an acceptable reliability of presented prediction method can be shown. It must be considered that the bed slope angle in real case is less than prediction graph.

The agreement between the results from prediction method with experimental and numerical results are summarized in Figure 5.

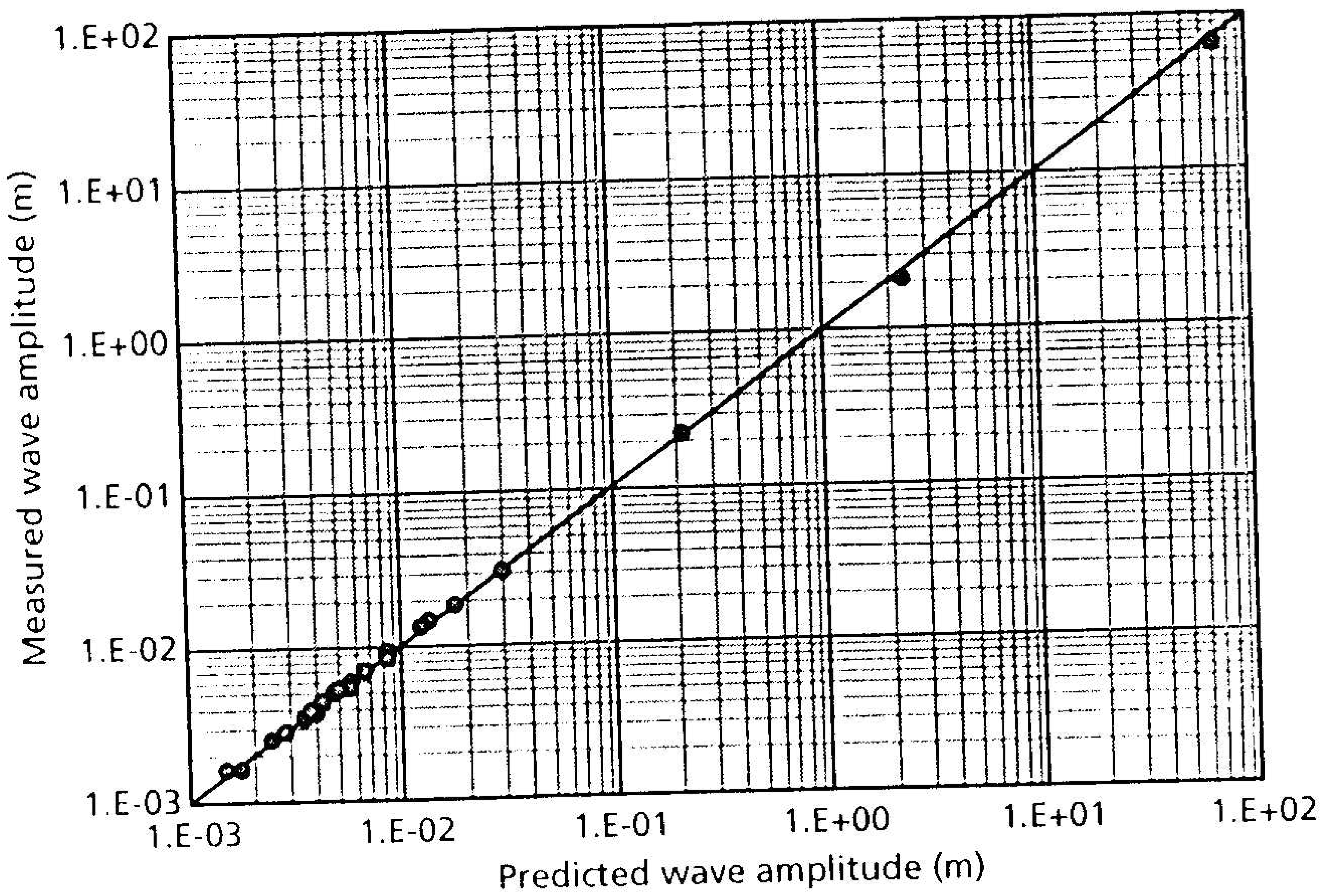

Figure 5: Accuracy of predicted impulsive wave amplitude vs results obtained by experiments, numerical models and real cases

5. Conclusion

A sensitivity analysis carried out for submerged landslide generated wave in dam reservoir using a higher order Boussinesq-type numerical model. The main geometric characteristics of submerged failure mass are investigated in dimensionless form. It is concluded that the main geometrical ratios which affected the impulse wave amplitude are as follow: the maximum thickness of sliding mass (T) over its length along the bed slope (B) (i.e. T/B), the initial submergence of center of failure mass (h_{0C}) over the sliding mass length (B) (i.e. h_{0C}/B). The main characteristic related to kinematics of sliding mass is assumed S_0, defined based on the initial acceleration and terminal velocity of sliding mass. Furthermore, the influence of bed slope is investigated on the impulse wave amplitude, wave length and its propagation pattern. The results show that the increasing effect of sliding thickness on the wave height multiplied in shallower landslides. These effects are fully nonlinear particularly for steeper bed slope when the initial submergence of sliding block diminishes.

Lastly, a simple and applied approach for estimation of impulse wave amplitude is presented. The method is validated using several experimental data and well-known 3D numerical models, and good agreements were obtained. The maximum error of predicted values is about 5% and the reliability of prediction method is confirmed. In addition, the predictive method is applied in some real cases for submarine mass failure and the impulse wave amplitude is appraised and compared with well-known numerical models and a good agreement is obtained. The present method can be used as an applied and engineering utility for the first estimate of LGWs.

6. Acknowledgements

The financial support of Water Resources Management Organization, Ministry of Power of the Islamic Republic of Iran is appreciated (Project number: DAM1-84010). Financial assistance was also provided partly by the Research Office of Sharif University of Technology, Iran.

Notations

ζ	= the water surface displacement from still water level scaled by a0 [-]
γ	= the slide mass density [$MT^{-2}L^{-2}$]
ε	= the nonlinearity ratio = a_0/h_0 [-]
θ	= the bed slope angle [deg.]
μ	= the frequency dispersion ratio = h_0/l_0 [-]
∇	= the horizontal gradient vector =$(\partial/\partial x, \partial/\partial y)$
α_0	= the initial acceleration of slide mass [LT^{-2}]
β	= the weighting parameter for determination of a characteristic depth [-]
A	= a two-component vector which is used in model derivation (Equation A11a)

[-]

a_0	= the impulse wave amplitude [L]
B	= the length of slide mass along the bed slope [L]
C_m	= Added mass coefficient [-]
C_d	= Drag coefficient [-]
g	= Acceleration due to gravity [LT-2]
h_0	= the characteristic water depth [L]
$h(x,y,t)$	= the depth of moving bottom boundary from still water level scaled by h_0 [-]
h_{0C}	= Initial still water depth at center point of sliding mass [L]
l_0	= the horizontal wavelength scale [L]
p	= the water pressure scaled by $\gamma_w a_0$ [-]
S_0	= the kinematics length sacale of sliding mass (Equation 11)[L]
t	= dimensionless time scaled by $l_0/(gh_0)^{1/2}$ [-]
T	= the maximum thickness of the slide mass [L]
u	= the vector of horizontal velocity components (u,v) scaled by $\varepsilon.(gh_0)^{1/2}$ [-]
ut	= the terminal velocity of slide mass [LT^{-1}]
u_0,u_1,u_2	= the dimensionless factors used for expanded form of u (Equation 7) [-]
w	= the velocity component in vertical direction scaled by $(\varepsilon/\mu).(gh_0)^{1/2}$ [-]
w_1, w_2	= the dimensionless factors used for expanded form of w (Equation 8) [-]
x,y	= the horizontal coordinates scaled by l0 [-]
z_a, z_b	= the elevations that the horizontal velocity components are described in them, scaled by h0 [-]
Z	= the characteristic variable depth which is a weighted average of two distinct water depths, z_a, z_b [-]
z	= the vertical coordinate scaled by h_0 [-]

References

[1]. Ataie-Ashtiani B., and Najafi-Jilani A., "A higher-order Boussinesq-type model with moving bottom boundary: applications to submarine landslide tsunami waves" Intl. Jl. for Numerical Methods in fluids, (in Press), 2006

[2]. Enet F., Grilli S.T., and Watts P., "Laboratory Experiments for Tsunami Generated by Underwater Landslides: Comparison with Numerical Modeling" 13th Intl. Conf. on Offshore and Polar Engrg, Honolulu, Hawaii, USA, pp 372-379, May 2003

[3]. Fritz H. M., Hager W. H., and Minor H. E., "Near field characteristics of landslide generated impulse waves", Jl of Waterway, Port, Coast. and Ocean Engrg, ASCE, Vol. 130, pp 287-302, 2004

[4]. Gobbi M. F., Kirby J. T., and Wei G.,"A fully nonlinear Boussinesq model for surface waves. II: Extension to O(kh4), Jl of Fluid Mechanics, Vol. 405, pp 181-210, 2000.

[5]. Goto, C., and Ogawa, Y., "Numerical method of tsunami simulation with the leap-frog scheme", Translated for the TIME project by N.Shuto, Dept. of Civil Engineering, Tohoku university, 1992.

[6]. Grilli S. T., Vogelmann S., Watts P., "Development of a 3D numerical wave tank for modeling tsunami generation by under water landslides" Jl of Engrg Analysis with Boundary Elements, Vol. 26, pp 301-313, 2002

[7]. Grilli S. T., and Watts P., "Under Water Landslide Shape, Motion, Deformation and Tsunami Generation" Jl of Intl Society of Offshore and Polar Engrs, ISBN 1-880653-5, pp 364-371 2003

[8]. Grilli S. T., and Watts P., "Tsunami Generation by Submarine Mass Failure. I: Modeling, Experimental Validation, and Sensitivity Analyses", Jl of Waterway, Port, Coast. and Ocean Engrg, ASCE, November/December, pp 283-297, 2005

[9]. Grilli S. T., Watts P., Kirby J. T., Fryer G. F., and Tappin D. R., "Landslide Tsunami Case Studies Using a Boussinesq Model and a Fully Nonlinear Tsunami Generation Model" Jl of Natural Hazards and Earth System Sciences, Vol. 3, pp 391-402, 1999

[10]. Heinrich P., "Nonlinear water waves generated by submarine and aerial landslides" Jl of Waterway, Port, Coast. and Ocean Engrg, ASCE, Vol. 118, pp 249-266, 1992

[11]. Imran, J., Parker, G., Lacat, J. and Lee, H., "1D Numerical model of muddy subaqueous and subaerial debris flows", Jl of Hyd. Engrg, November, pp 959- 968, 2001

[12]. Jiang L., and Leblond PH., "The coupling of a submarine slide and the surface waves which it generates", Jl of Geophysical Researches, Vol. 12, pp 731-744, 1992

[13]. Johnson J. W., and Bermel K. J., "Impulsive waves in shallow water as generated by falling weights", Trans. of American Geophysical Union, Vol. 30, pp 223-230, 1949

[14]. Kamphuis, J.W., Bowering, R.J. "Impulse waves generated by landslides". Proc. 12th Coastal Engineering Conference, ASCE, Vol. 1, pp 575-588, 1972

[15]. Lynett P., and Liu P. L., "A numerical study of submarine-landslide-generated

waves and run-up", Phil. Trans. Royal society, London, U.K..A458, pp 2885-2910, 2002

[16]. Lynett P., and Liu P. L.-F., "A multi-layer approach to wave modeling", Proc. Royal Society, London, A, Vol. 460, pp 2637-2669, 2004.

[17]. Mader, C. L., "Numerical simulation of tsunamis", Tsunami research report of university of Hawaii, Honolulu, Hawaii, University of Geophysics, 1973

[18]. Miller D. J., "Giant waves in Lituya Bay, Alaska", U.S. Geological Survey, Prof. Papers, 354-C, pp 51-83, 1960

[19]. Noda, E. K., "Water waves generated by a local surface disturbance", Jl of Geophysical Research, Vol. 76(30), pp 7389-7400, 1971.

[20]. Nwogu O., "An alternative form of Boussinesq equations for near shore wave propagation" Jl of Waterway, Port, Coast. and Ocean Engrg, ASCE, Vol. 119(6), pp 618-638, 1993

[21]. Ogawa T., "Notes on the volcanic and seismic phenomena in the volcanic district of Shimabara, with a report on the earthquake of December 8, 1922", Mem. of College of Society, Kyoto Imperical University, Ser. B, Vol. 1, (2), 1924.

[22]. Panizzo A., Girolamo P. D., Risio M. D., Maistri A., and Petaccia A., "Great landslide events in Italian artificial reservoirs", Jl of Natural Hazards and Earth System Sciences, Vol. 5, pp 733-740, 2005

[23]. Peregrine D. H., "Long waves on a beach" Jl of Fluid Mechanics, Vol. 27, pp 815-827, 1967

[24]. Prins, J.E. "Characteristics of waves generated by a local disturbance". Trans. American Geophysical Union, , Vol. 39(5), pp 865-874, 1958

[25]. Raney D. C., and Butler H. L., "A numerical model for predicting the effects of landslide generated water waves" U.S. Army Engrg Waterway and Reservoir Report, No. H-75-1, 1975

[26]. Rzadkiewicz, S.A., Mariotti, C., and Heinrich, P., "Numerical simulation of submarine landslides and their hydraulic effects", Jl of Waterway, Port, Coast. and Ocean Engrg, ASCE, July/August, pp 149-157, 1997

[27]. Slingerland R. L., and Voight B., "Occurrence, properties and predictive models of landslide generated water waves", In Developments in Geotechnical Engineering 14B, Rockslides and Avalanches, 2, Ed. B. Voight, Elsevier, pp 317-397, 2000

[28]. Synolakis, C. E., Bardet, J, P, Borrero, J. C., Davies, H. L., Okal, E. A., Solver, E. A., Sweet, S., and Tappin, D. R., "The slump origin of the Papua New Guinea tsunami", Royal society of London, A, 458, pp 763-789, 2002.

[29]. Titov V. V., "Numerical modeling of long wave run-up" Ph.D. thesis, University of Southern California, Los Angeles, California, 141 pp, 1997

[30]. Walder J. S., Watts P., Sorensen O. E., and Janssen K., "Tsunami Generated by Sub Arial Mass Flows" Jl of Geophysical Research, Vol. 108, No. B5. 2236, pp EPM 2:1-2:19, 2003

[31]. Watts P., "Wave maker curves for tsunami generated by underwater landslide" Jl of Waterway, Port, Coast. and Ocean Engrg, ASCE, Vol. 12(3), pp 127-137, 1998

[32]. Watts P., Grilli S. T., Kirby J. T., Fryer G. F., and Tappin D. R., "Landslide Tsunami Case Studies Using a Boussinesq Model and a Fully Nonlinear Tsunami Generation Model" Jl of Natural Hazards and Earth System Sciences, Vol. 3, pp 391-402, 2003

[33] Watts P., and Grilli S. T., Tappin, D.R., and Fryer, G. J., "Tsunami Generation by Submarine Mass Failure. II: Predictive Equations and Case Studies", Jl of Waterway, Port, Coast. and Ocean Engrg, ASCE, November/December, pp 283-297, 2005

[34]. Wiegel R. L., "Laboratory studies of gravity waves generated by the movement of a submarine body", Trans. of American Geophysical Union, Vol. 36, pp 759-774, 1955